

# Self-Assembled Magnetic Surface Swimmers

A. Snezhko,<sup>1</sup> M. Belkin,<sup>1,2</sup> I.S. Aranson,<sup>1</sup> and W.-K. Kwok<sup>1</sup>

<sup>1</sup>*Materials Science Division, Argonne National Laboratory, 9700 South Cass Avenue, Argonne, IL 60439*

<sup>2</sup>*Illinois Institute of Technology, 3101 South Dearborn Street, Chicago, IL 60616*

(Dated: December 7, 2008)

We report studies of novel self-assembled magnetic surface swimmers (magnetic snakes), formed from a dispersion of magnetic microparticles on the liquid/air interface and energized by an alternating magnetic field. We show that under certain conditions the snakes spontaneously break the symmetry of surface flows and turn into self-propelled objects. Parameters of the driving magnetic field tune the propulsion velocity of these snake-like swimmers. We find that the surface flows symmetry can be also broken in a controlled fashion by attaching a large bead to a magnetic snake (bead-snake hybrid), transforming it into a robust self-locomoting entity. Observed phenomena have been successfully described by phenomenological model based on the amplitude equation for surface waves coupled to the large-scale hydrodynamic mean flow equation.

PACS numbers: 87.19.ru; 43.35.Lf; 75.50.Tt; 47.63.Gd

Fundamental mechanisms governing locomotion at macro- and micro-scale are attracting enormous attention in the physics community [1–10]. The interest is driven by the need of understanding how the biological organisms propel themselves in various environments and by the growing demand for design of artificial externally controlled structures capable of performing useful tasks at the microscale, including targeted cargo delivery [11, 12] or stirring in microfluidic devices [13]. Several concepts of low-Reynolds number micro-swimmers were proposed, including three-sphere swimmer [3] and DNA-linked colloidal magnetic nano-particles swimmer [5]. Typically, the propulsion mechanism is associated with the breaking of a time-reversal symmetry of reciprocal motion of swimmer’s body [14], such as rotation of helical flagella by motile bacteria.

In our earlier studies [15, 16] we reported self-assembly of magnetic microstructures (magnetic snakes) from a dispersion of magnetic microparticles suspended on the water-air interface and subjected to a vertical alternating magnetic field. These structures appear due to the coupling between fluid’s surface deformations and the collective response of particles on an external alternating magnetic field. In the course of particle’s magnetic moment alignment with the external field, the particles produce local deformations of the water surface, thereby affecting neighboring particles. These deformations bring particles close enough that the head-to-tail dipole-dipole attraction overcomes the repulsion caused by the external field. As a result, chains of particles are formed with the resulting magnetic moment pointing along the chains. The chains produce wave-like local motion facilitating the self-assembly process (parallel to the surface of the water component of the magnetic field further promotes chain formation, see for detail Ref. [16]). The snakes consist of sections (segments) formed by ferromagnetically aligned chains of microparticles. The length of the segments is defined by the surface wavelength (two segments

per wavelength). The segments, however, are always antiferromagnetically ordered [17–19].

In this Letter we report a discovery of a conceptually new type of self-assembled magnetic surface swimmers that form in the same system, magnetic microparticles at the water/air interface. We find that the magnetic snakes under certain conditions *spontaneously break the symmetry* of surface flows and turn into self-propelled entities. Alternatively, another type of swimmers is realized via controlled breaking of the surface flows symmetry by attaching a bead to one of the snake’s ends (bead-snake hybrid). Both types of magnetic swimmers are unique due to unusual mechanism of self-propulsion exploiting symmetry breaking of self-generated surface flows and intrinsic antiferromagnetic nature of the swimmer’s structure. The magnetic field parameters can be used to control the propulsion velocity and the structure of the swimmers. Our phenomenological model successfully reproduced observed experimental observations.

Our experimental setup is similar to that reported in [15], however with a number of modifications: more than a 4-fold increase in the area of experimental cell and in the bore of the coils, and considerably increased values of accessible magnetic fields. A glass beaker (10 cm in diameter) is filled with water and placed in the center of precision Helmholtz magnetic coils (13 cm in diameter) capable of creating vertical magnetic fields up to 170 Oe. Magnetic microparticles (90 micron Nickel spheres) are suspended on the surface of water and supported by surface tension. Particles positions are monitored by a high-speed camera mounted on an optical microscope stage. A homogeneous vertical sinusoidal magnetic field  $\mathbf{H} = H_0 \sin(2\pi ft)\mathbf{z}_0$  with the amplitude  $H_0$  and the frequency  $f$  was applied.

The snake is accompanied by four large symmetric hydrodynamic vortices located at the opposite ends of the snake [17] (vortex quadrupole). As a result, the two ends of the snake represent miniature engines pumping

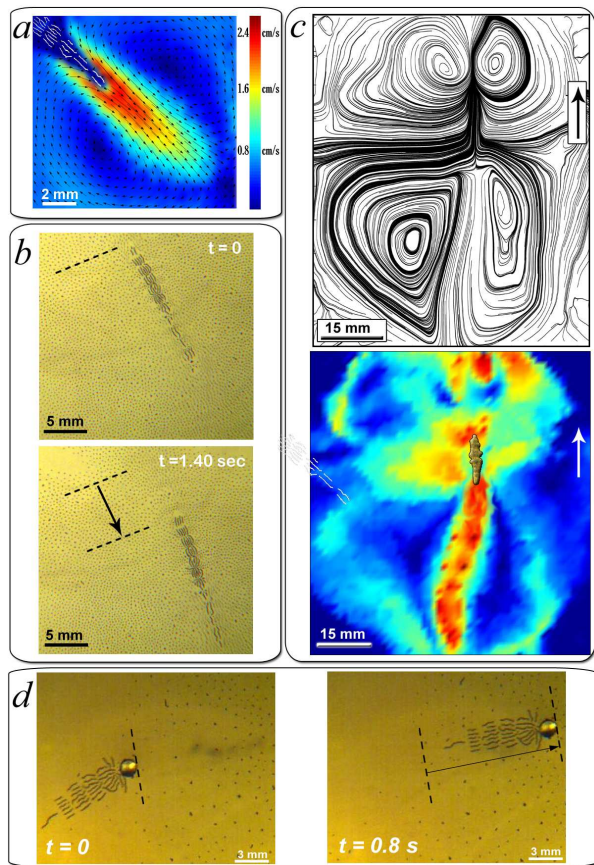


FIG. 1: (Color online) Magnetic swimmers generated by a vertical alternating magnetic field. (a) Surface flow velocity field in the vicinity of the snake’s tail. Arrows depict the surface velocity field obtained by PIV and the background colors show relative magnitudes of flow velocities. (b) Self-propelled magnetic swimmer energized by a 100 Oe, 140 Hz vertical magnetic field. (c) The vortex structure of a self-propelled snake. Arrow shows the direction of swimming. Bottom image illustrates the amplitude of the surface flows around the swimming snake. Dark blue color corresponds to the low velocities of flows; long jet-stream emanates from one of the snake’s tails. (d) Self-propelled snake-particle hybrid,  $f=80$  Hz,  $H_0=100$  Oe, 1.5 mm spherical glass bead is used.

the surrounding liquid in opposite directions. Figure 1a shows the flow created by one of such “engines” obtained by the particle image velocimetry (PIV). The flow generated by the snake could be as fast as a few centimeters per second and is controlled by the frequency and the amplitude of external magnetic field [17]. In the low frequency case (frequency of the external magnetic field is below about 100 Hz), both “engines” are identical. Consequently, the flows are exactly compensated and the snake is at rest (no translational movement in x-y plane). However, we have found that as the frequency of the magnetic field is increased, the stationary snake transforms into a self-propelled magnetic swimmer via spontaneous symmetry breaking of the balance between the

“engines”, and, consequently, of the quadrupole vortex structure. Experimental observation of such a behavior is illustrated in Fig. 1b and movies 1 and 2 [18]. There is no sharp transition frequency but a transition region, about 30 Hz wide around 120 Hz. Once transformed into a self-propelled swimmer, the snake tends to swim on a straight line unless it collides with the container wall or other snake. Collisions with the container wall typically lead to a subsequent destruction of the snake and reassembly of another snake at a different location. Depending on the initial density of magnetic particles at the surface of liquid, more than one self-propelled snake may appear at the same time (the higher the density, the more snakes could be induced), see movie 2 [18]. In the case of multiple swimmers, the shape, the length, and sometimes even the total number of snakes may vary. A closer look at a mechanism of self-propulsion of the initially motionless snake reveals a drastic spontaneous change of the flow pattern. Figure 1c shows the surface flow structure of the swimming snake. Apparently, as the frequency of the magnetic field is increased, the snake develops highly asymmetric vortex structure. One pair of the vortices associated with one of the snake’s tails becomes stronger than another meaning that one of the “engines” becomes more powerful. Resulting net difference in the engines power propels the snake.

Bottom image in Fig. 1c displays the amplitude of flow velocity in the vicinity of the magnetic swimmer: long jet-stream emanating from one of the snake’s tails reveals the uncompensated flow generated by the swimmer. In the course of our experiments, the self-propelled snakes appear at random locations and then swim on straight trajectories in the direction determined by initial orientations, see movie 2. Whereas the velocity of the snakes could be tuned by parameters of external magnetic field (the higher frequencies produce more rapid swimmers), their propulsion direction could not be easily controlled by external magnetic field in contrast to artificial magnetic swimmers assembled from DNA-linked magnetic nanoparticles [5]. While in the later case the swimmer simply moves along a static in-plane magnetic field, self-propelled snakes react completely differently to the external in-plane fields due to their *intrinsic anti-ferromagnetic nature* [15, 16, 19] resulting in zero net magnetic moment of the structure.

We have found experimentally that it is also possible to create a self-propelled magnetic swimmer from a stationary snake even below the threshold of self-propulsion instability. It can be done by placing a large glass or polystyrene bead (1-2 mm) near one of the snake’s tails. The snake often self-attaches to the bead forming a robust swimming bead-snake hybrid. The bead suppresses the vortex flow at one of the snake’s tails giving rise to uncompensated flow that propels the swimmer (see movies 3 [18]). Figure 1d shows a sequence of snapshots illustrating the motion of the structure with a 1.5 mm spherical

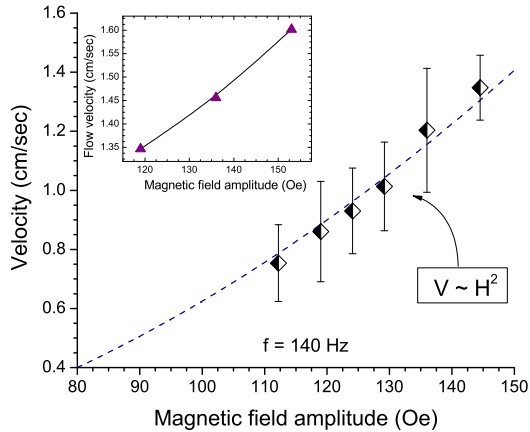


FIG. 2: (Color online) Mean swimming velocity of the snake-bead hybrid vs amplitude of magnetic field at  $f = 140$  Hz. Dashed line is a fit to quadratic dependence of the swimmer velocity on the amplitude of external field,  $V \sim H^2$ . *Insert*: flow velocity at the tail of the stable snake generated at  $f = 140$  Hz. The swimming velocity is of the same order as maximum flow velocity of a stationary snake.

glass bead. In our experimental setup we were able to create such stable snake-particle hybrids moving in circles along the container wall (see movies 4 and 5).

Figure 2 shows swimming velocity of the snake-particle hybrid vs external magnetic field amplitude. The velocity closely follows the quadratic dependence on the external field amplitude  $H$  as one would anticipate for a streaming flow induced by an oscillating object (compare to Rayleigh streaming) [20],  $V \sim fA^2/a_0$ , where  $A$  is the amplitude of vertical oscillations of the tail which is proportional to amplitude of magnetic field  $H$ , and  $a_0$  is the typical size of the snake segment (of the order of wavelength  $\lambda$ ). We find that the swimming velocity is of the same order as the velocity of the stream generated by the stationary snake (see insert to Fig. 2).

To obtain insights into mechanism of self-propulsion, we extended a phenomenological model reported in Ref. [17]. The model is formulated in terms of the paradigm Ginzburg-Landau type equation for parametric surface waves coupled to the conservation law for the magnetic particle density and the equation for large-scale mean flow. To describe the mechanism of the spontaneous symmetry breaking of the surface flow structure and the formation of self-propelled swimmers, last two terms in Eq.

(1) has been introduced into the model (Eqs. (1)-(3)).

$$\begin{aligned} \partial_t \psi + (\mathbf{v} \nabla) \psi = & \\ - (1 - i\omega) \psi + (\varepsilon + ib) \nabla^2 \psi - |\psi|^2 \psi + \gamma \psi^* \phi(\rho) & \\ + i\alpha_1 \psi^* (\nabla \psi)^2 + \alpha_2 \psi |\nabla \psi|^2 & \end{aligned} \quad (1)$$

$$\partial_t \rho + \nabla(\rho \mathbf{v}) = D \nabla^2 \rho - \beta \nabla(\rho \nabla |\psi|^2) \quad (2)$$

$$\partial_t \mathbf{v} + (\mathbf{v} \nabla) \mathbf{v} + \frac{\nabla p}{\rho_f} = \nu \nabla^2 \mathbf{v} + \mathbf{F} \quad (3)$$

In Eq. (1) the field  $\psi$  describes the complex amplitude of surface waves. Forcing by external alternating magnetic field (parametric driving) is described by the term  $\gamma \psi^* \phi(\rho)$ , terms  $|\psi|^2 \psi$  and  $\varepsilon \nabla^2 \psi$  account for nonlinear damping and viscous dissipation (see for detail [21]). The function  $\phi(\rho)$  in the driving term accounts for saturation of forcing for higher values of particle density  $\rho$ . Conservation law for magnetic particles' density  $\rho$  is represented by Eq. (2), where  $D$  is a diffusion coefficient and advection term (which describes advection of particles by waves) has amplitude  $\beta$ . Eq. (3) is a Navier-Stokes equation for evolution of large-scale hydrodynamic velocity field  $\mathbf{v}$ .  $p$  is the pressure and  $\rho_f$  and  $\nu$  are the fluid's density and viscosity respectively. We assume that the characteristic scale of the hydrodynamic field  $\mathbf{v}$  is much larger than that associated with the surface waves. It allows considering the situation when the large-scale flow  $\mathbf{v}$  is purely two-dimensional which leads to a considerable simplification of Eq. (3) by introducing a stream func-

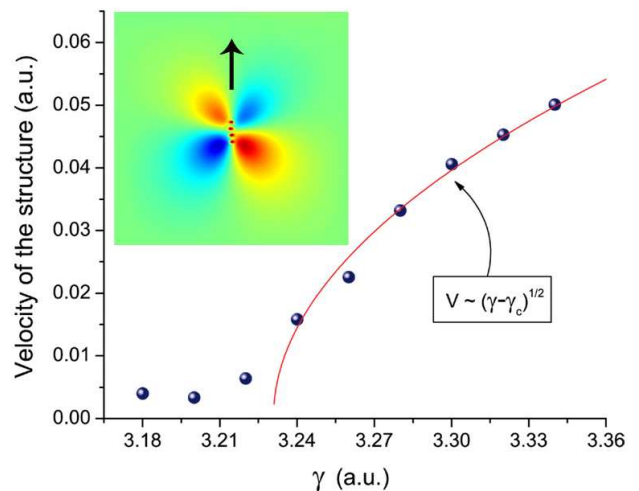


FIG. 3: (Color online) Numerical studies of self-propelled snake. Onset of the snake's symmetry breaking and swimming. Solid line is a fit to  $(\gamma - \gamma_c)^{1/2}$  dependence. *Inset*: spontaneous symmetry breaking of the snake's quadrupole vortex flows (colors represent the values of stream function  $\Omega$ ) obtained from Eqs. (1)-(3). Arrow shows the direction of swimming, note the asymmetry between vortex pairs. Parameters in Eqs. (1)-(3) are:  $\varepsilon = 1, b = 5, \gamma = 3.32, D = 0.2, \beta = 60, \omega = 3, \alpha_1 = 10000, \alpha_2 = 5000, \nu = 1.5$  in domain of  $200 \times 200$  dimensionless units.

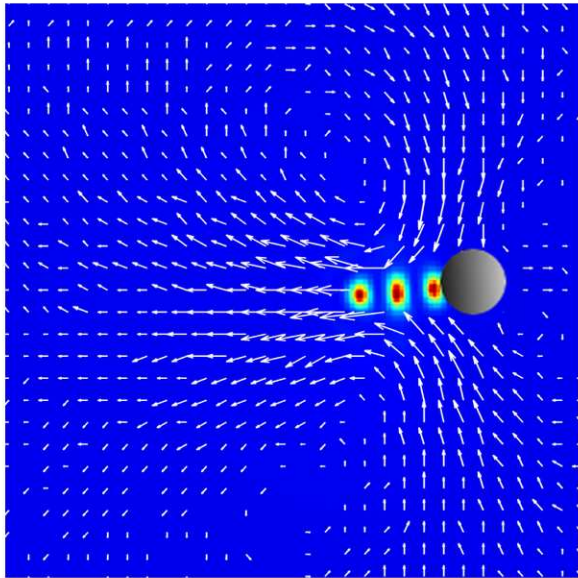


FIG. 4: (Color online) Velocity field of snake-particle hybrid (arrows), colors show the value of  $|\psi|^2$ . Simulation performed at  $\omega = 2.95, \gamma = 3.20$ . Gray circle in the image depicts the area where the forcing term  $\mathbf{F}$  in Eq. (3) is suppressed.

tion  $\Omega$ ,  $v_x = \partial_y \Omega$ ,  $v_y = -\partial_x \Omega$ . External driving averaged over one period is taken into account by the vector force  $\mathbf{F}$ , whose form from the symmetry reasons is chosen to be  $\mathbf{F} = \zeta(\psi^* \nabla \psi - \psi \nabla \psi^*)$ . The last two terms in Eq. (1) are formally higher order compared to other terms (in the framework of the Ginzburg-Landau theory). Our simulations revealed that these two terms are responsible at least for two non-trivial effects: (i) they provide structural rigidity of the snake and control its length to width ratio. Without these terms the snake appears to be compressed by flows generated from the tails (segments in the center become much wider than at the tails). (ii) For large enough magnitude of  $\alpha_{1,2}$  the snake exhibits symmetry-breaking instability and the onset of spontaneous swimming similar to that observed in experiment.

Figure 3 features numerical solution of Eq.(1)-(3). The model captures the onset of symmetry-breaking instability of the quadrupole vortex structure when the snake develops spontaneous swimming (see also movie 6). Inset in Fig. 3 displays the stream function of the moving snake as obtained from simulations. One sees a profound asymmetry of the surface vortex flows developed by the snake. The swimming velocity exhibits a square root dependence on the external driving  $\gamma$ , the hallmark of symmetry breaking instability (solid line in Fig. 3).

Our model has also successfully captured the translational motion of the snake when the flows were intentionally suppressed at one of the snake's ends (see movie 7). In order to perform simulations of snake-bead hybrid, we modeled the influence of spherical bead by introduction

of an attenuation of forcing term,  $\mathbf{F}$ , in the vicinity of one of the snake's tails. A typical flow structure in the vicinity of the snake-particle hybrid as obtained from the simulations is shown in Fig. 4.

To conclude, we have found conceptually new realization of self-assembled magnetic swimmers. Being self-assembled from a dispersion of magnetic particles in the system with complex (magnetic, hydrodynamic) interactions, the swimmers have the ability to exhibit propulsion due to spontaneous breaking of symmetry of quadrupole vortex flows. We show that self-assembled magnetic swimmers can be also realized by controlled breaking of the flow symmetry leading to robust snake-bead hybrids. Our results yield fundamental insights into mechanisms of self-assembly and locomotion in non-equilibrium systems with complex interactions between the particles, and also provide an interesting opportunity to model surface locomotion on living organisms [22]. The snake-bead hybrids also open new intriguing opportunity for functionalization of the snake's head for the purpose of targeted delivery or transport. This research was supported by US DOE, Grant # DE-AC02-06CH11357.

- 
- [1] J.E. Avron, O. Gat, and O. Kenneth, Phys. Rev. Lett. **93**, 186001 (2004)
  - [2] R. Golestanian and A. Ajdari, Phys. Rev. Lett. **100**, 038101 (2008)
  - [3] A. Najafi, R. Golestanian, Phys. Rev. E **69**, 062901 (2004)
  - [4] C.M. Pooley, A.C. Balazs, Phys. Rev. E **76**, 016308 (2007)
  - [5] R. Dreyfus et al., Nature **437**, 862-865 (2005)
  - [6] F. Y. Ogrin, P. G. Petrov, C. P. Winlove, Phys. Rev. Lett. **100**, 218102 (2008)
  - [7] D.C. Rapaport, Phys. Rev. Lett. **99**, 238101 (2007)
  - [8] J.E. Avron, O. Raz, New Jour. of Phys. **10**, 063016 (2008)
  - [9] A.M. Leshansky and O. Kenneth, Phys. of Fluids **20**, 063104 (2008)
  - [10] R. Trouilloud, T. S. Yu, A.E. Hosoi, E. Lauga, Phys. Rev. Lett. **101**, 048102 (2008)
  - [11] J. Edd et al., Proceed. of the IEEE/RSJ. Intl. Conf. on Intelligent Robots and Systems, **3**, 2583-2588 (2003)
  - [12] O. Raz, A.M. Leshansky, Phys. Rev. E **77**, 055305(R) (2008)
  - [13] S.T. Chang et al., Nat. Mater, **6**, 235-240 (2007)
  - [14] E. M. Purcell, Am. J. Phys. **45**, 3 (1977)
  - [15] A. Snezhko, I.S. Aranson, W.-K. Kwok, Phys. Rev. Lett. **96**, 078701 (2006)
  - [16] A. Snezhko, I. S. Aranson, and W.-K. Kwok, Phys. Rev. E **73**, 041306 (2006)
  - [17] M. Belkin, A. Snezhko, I. S. Aranson, and W.-K. Kwok, Phys. Rev. Lett. **99**, 158301 (2007)
  - [18] See EPAPS Document No. and ANL website <http://mti.msd.anl.gov/highlights/snakes/> for movies illustrating dynamic self-assembled magnetic swimmers.
  - [19] A. Snezhko, I.S. Aranson, Phys. Lett. A **363**, 337 (2007)
  - [20] N. Riley, Quart. Journ. Mech. and Appl. Math., **19**, 461 (1966); M. Belovs and A. Cebers, Phys. Rev. E. **73**,

- 051503 (2006)
- [21] I.S. Aranson and L.S. Tsimring, Rev. Mod. Phys. **78**,641 (2006).
- [22] J. W.M. Bush and D. L. Hu, Annu. Rev. Fluid Mech. **38**, 339 (2006)